

AD-A263 020



1



National
Defence

Défense
nationale



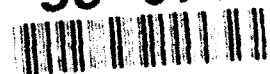
AN IMPROVED KALMAN FILTER EXCISOR FOR SUPPRESSING NARROWBAND GAUSSIAN NOISE INTERFERENCE

by

Brian Kozminchuk



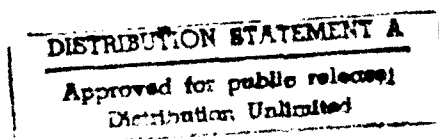
93-07987



36PC

DEFENCE RESEARCH ESTABLISHMENT OTTAWA
TECHNICAL NOTE 92-28

Canada



November 1992
Ottawa

93 4 30 040



National
Defence

Défense
nationale

AN IMPROVED KALMAN FILTER EXCISOR FOR SUPPRESSING NARROWBAND GAUSSIAN NOISE INTERFERENCE

by

Brian Kozminchuk

*Communications Electronic Warfare Section
Electronic Warfare Division*

DEFENCE RESEARCH ESTABLISHMENT OTTAWA

TECHNICAL NOTE 92-28

PCN
041LK11

November 1992
Ottawa

ABSTRACT

This technical note presents an improved Kalman filter excisor for dealing with narrow-band Gaussian noise. For this type of interference, both envelope and phase vary with time. Since the Kalman filter approach is close to optimum for interferers with constant or very slowly varying envelopes, performance for the narrowband Gaussian noise case will be significantly less than optimum. Ways and means of improving the performance by up to 5 dB are presented. These include the use of an alternate filtering approach to estimate the envelope to counter group delay effects, and phase-smoothing to suppress some of the additional noise caused by temporary loss of lock by the Kalman filter during those instants when the envelope changes sign.

RÉSUMÉ

Cette note technique présente un algorithme basé sur l'utilisation d'un filtre de Kalman pour l'excision de bruits gaussiens à bande étroite, lesquels possèdent une enveloppe et une phase variant rapidement dans le temps. Etant donné que le filtre de Kalman est quasi optimal pour des signaux interférents à enveloppe variant très lentement, la performance diminue considérablement lorsque l'interférence est un bruit gaussien à bande étroite. Une méthode pour améliorer la performance de 5 dB est proposée. Cette méthode inclut l'utilisation d'un autre filtre pour estimer l'enveloppe du signal dans le but de compenser l'effet du délai de groupe, ainsi que l'utilisation d'un filtre pour adoucir les brusques changements de phase causés par les pertes de synchronisation du filtre de Kalman, lesquels se produisent lorsque l'enveloppe du signal change de signe.

DTIC QUALITY INSPECTED 4

Accession For	
NTIS GRA&I	<input checked="" type="checkbox"/>
DTIC TAB	<input type="checkbox"/>
Unannounced	<input type="checkbox"/>
Justification	
By	
Distribution/	
Availability Codes	
Dist	Avail and/or Special
A-1	

EXECUTIVE SUMMARY

This technical note presents an improved Kalman filtering approach that is used for filtering narrowband Gaussian noise interference out of direct sequence spread spectrum signals. These signals are used extensively in military communication systems. The technique described herein applies equally to both Electronic Support Measures (ESM) systems and direct sequence spread spectrum communication systems. In the former application, the ESM system may be attempting to intercept the spread spectrum signal, but the narrowband interference may be hampering this effort. In the latter application, the spread spectrum communication system may require additional assistance to suppress the interference. Since the open literature has been devoted to this latter case, the material presented here focuses on this application.

One of the attributes of direct sequence spread spectrum communication systems is their ability to combat interference or intentional jamming by virtue of the system's processing gain inherent in the spreading and despreading process. The interference can be attenuated by a factor up to this processing gain. In some cases the gain is insufficient to effectively suppress the interferer, leading to a significant degradation in system performance as manifested by a sudden increase in bit error rate. If the ratio of interference bandwidth to spread spectrum bandwidth is small, the interference can be filtered out to enhance system performance. However, this is at the expense of introducing some distortion onto the signal. This process of filtering is sometimes referred to as interference excision.

The Kalman filtering approach is based on the digital phase-locked loop Kalman filter and is close to optimum for demodulating an FM-type of interferer. Because the interference is assumed to be much stronger than either the signal or noise, the Kalman filter locks onto the interference and produces an estimate of the phase and envelope of the interference.

In the case of narrowband Gaussian noise, the envelope varies significantly. The time-varying nature of the envelope leads first to an unknown group delay in the envelope estimate if an IIR filter is used and, second, to sudden phase changes when the envelope changes sign; for this latter situation, the Kalman filter loses temporary lock in its phase-tracking and must re-acquire the interference. Both the group delay and phase-tracking problems contribute to an excess amount of residual interference at the output of the interference canceller, resulting in an overall degradation in performance. To combat the unknown group delay caused by an IIR filter, a linear phase FIR filter with known group delay is used in the envelope estimator. To combat the excess noise caused by

the sudden phase changes, additional phase smoothing is incorporated in the Kalman filter. Through computer simulation, it is shown that both enhancements contribute to an overall improvement in performance of 4 to 5 dB for interference bandwidths ranging from 1% to 5% of the chip rate.

TABLE OF CONTENTS

ABSTRACT/RÉSUMÉ	iii
EXECUTIVE SUMMARY	v
TABLE OF CONTENTS	vii
LIST OF FIGURES	ix
1.0 INTRODUCTION	1
2.0 COMMUNICATIONS MODEL	1
3.0 INTERFERENCE ESTIMATOR	4
4.0 NARROWBAND GAUSSIAN NOISE INTERFERENCE	5
4.1 FILTER LAG EFFECTS	5
4.2 PHASE-NOISE EFFECTS	7
5.0 CONCLUSIONS	25
REFERENCES	REF-1

LIST OF FIGURES

Figure 1:	Spread spectrum communications model.	2
Figure 2:	Block diagram of the interference estimator.	4
Figure 3:	Level of interference suppression \mathcal{S} as a function of d for several lowpass filter bandwidths. The interference is narrowband Gaussian noise of bandwidth 0.02 Hz.	8
Figure 4:	An example of a portion of the envelope I_n and its estimate \hat{I}_n when the filter is of the Butterworth type of bandwidth $B_{LPF} = 0.20$ Hz with $d = 0.30$ rad./sec./volt and interference bandwidth $B_i = 0.02$ Hz. . . .	9
Figure 5:	An example of a portion of the interference i_n and its estimate \hat{i}_n when the filter is of the Butterworth type of bandwidth $B_{LPF} = 0.20$ Hz, $d = 0.30$ rad./sec./volt and interference bandwidth $B_i = 0.02$ Hz. . . .	10
Figure 6:	An example of a portion of the envelope I_n and its estimate \hat{I}_n when the filter is of the Butterworth type of bandwidth $B_{LPF} = 0.40$ Hz with $d = 0.30$ rad./sec./volt and interference bandwidth $B_i = 0.02$ Hz. . . .	11
Figure 7:	An example of a portion of the interference i_n and its estimate \hat{i}_n when the filter is of the Butterworth type of bandwidth $B_{LPF} = 0.40$ Hz, $d = 0.30$ rad./sec./volt and interference bandwidth $B_i = 0.02$ Hz. . . .	12
Figure 8:	Modified interference estimator of Fig. 2 when the low pass filter is a linear phase FIR filter.	13
Figure 9:	Comparison of the interference suppression levels \mathcal{S} produced by a 7-tap FIR filter and 4 th order Butterworth filter when $B_i = 0.02$ Hz, $B_{LPF} = 0.20$ Hz, and $E_b/N_0 = 12$ dB.	14
Figure 10:	An example of a portion of the envelope I_{n-D} and its estimate \hat{I}_{n-D} when the filter is of the linear phase FIR type of bandwidth $B_{LPF} = 0.20$ Hz with $d = 0.30$ rad./sec./volt and interference bandwidth $B_i = 0.02$ Hz. . . .	15
Figure 11:	An example of a portion of the interference i_{n-D} and its estimate \hat{i}_{n-D} when the filter is of the FIR type of bandwidth $B_{LPF} = 0.20$ Hz, $d = 0.30$ rad./sec./volt and interference bandwidth $B_i = 0.02$ Hz.	16
Figure 12:	Interference suppression level \mathcal{S} as a function of d for several interference bandwidths, B_i , ranging from 0.01 Hz to 0.04 Hz, with $B_{LPF} = 0.20$ Hz. . . .	17

Figure 13: Interference estimator when phase-smoothing is being used.	18
Figure 14: An example of the phase θ_n and its Kalman filter estimate $\hat{\theta}_{n n-1}$, with interference bandwidth $B_i = 0.02$ Hz and $d = 0.30$ rad./sec./volt. . . .	19
Figure 15: An example of the phase θ_n and a 7-point smoothed version $\hat{\theta}'_{n-D}$ of its Kalman filter estimate $\hat{\theta}_{n n-1}$, with interference bandwidth $B_i = 0.02$ Hz and $d = 0.30$ rad./sec./volt.	20
Figure 16: An example of a segment of interference with and without phase smoothing; interference bandwidth $B_i = 0.02$ Hz and $d = 0.30$ rad./sec./volt. . . .	21
Figure 17: Interference suppression level S as a function d for several interference bandwidths, B_i , ranging from 0.01 Hz to 0.05 Hz, with $B_{LPF} = 0.20$ Hz. . . .	22
Figure 18: Bit error rate for the case of narrowband Gaussian noise with bandwidths B_i ranging from 0.01 Hz to 0.05 Hz, using the optimum values of d obtained from Fig. 17, and an FIR filter with no averaging on the phase estimate $\hat{\theta}_{n n-1}$	23
Figure 19: Bit error rate for the case of narrowband Gaussian noise with bandwidths B_i ranging from 0.01 Hz to 0.05 Hz, using the optimum values of d obtained from Fig. 17, and an FIR filter with 7-point averaging on the phase estimate $\hat{\theta}_{n n-1}$	24

1.0 INTRODUCTION

Several reports have been written by the author on the subject of interference suppression of narrowband interference from direct sequence spread spectrum communications signals using a Kalman filtering technique [1, 2, 3]. The first two reports dealt with interferers which were of the constant envelope type for which the Kalman filtering technique provides close to optimum performance. The last report evaluated the Kalman filter excisor for the case of narrowband Gaussian noise—a more difficult type of interference because both the envelope and phase vary with time. This technical note presents an improved excisor to deal with the more difficult narrowband Gaussian noise interference problem as discussed in [3].

The outline of the technical note is as follows. Section 2.0 presents the communications model used in the simulations. Section 3.0 describes the basic interference estimator which was used in the previous reports [1, 2, 3] and to which enhancements will be made to improve the performance for narrowband Gaussian interference. Section 4.0 presents the problem to be solved. These include two things: (a) the effects of group delay caused by the low pass filter used to estimate the envelope; and, (b) the additional phase noise caused by a loss of phase-lock in the Kalman filter when the envelope changes sign. Enhancements to the system are presented and evaluated. Finally, Section 5.0 concludes the technical note, suggesting areas for further research.

2.0 COMMUNICATIONS MODEL

The basic elements of the BPSK PN spread spectrum receiving system are shown in Fig. 1. The received waveform $r(t)$, consisting of a spread spectrum signal, additive white Gaussian noise, and narrowband interference is applied to a bandpass filter with the transfer function $H_{bp}(f)$, whose output is defined as

$$u(t) = s(t) + n(t) + i(t). \quad (1)$$

The bandpass filter $H_{bp}(f)$, for the application considered here, is assumed to be a filter matched to a chip and centered at the carrier angular frequency ω_0 of the spread spectrum signal. The spread spectrum signal is defined as

$$s(t) = a(t) \cos(\omega_0 t) \quad (2)$$

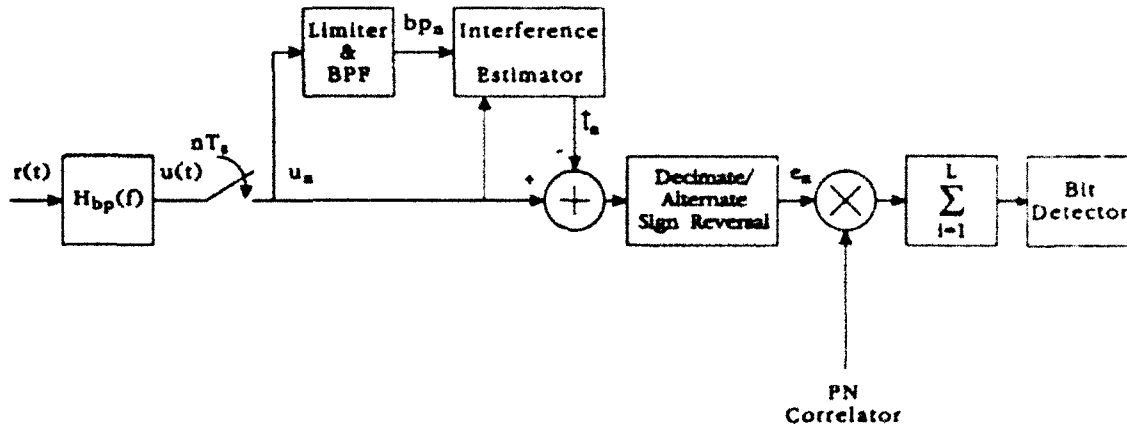


Figure 1: Spread spectrum communications model.

where

$$a(t) = \sum_k D_k b_k(t - kT_b). \quad (3)$$

In Eq. (3), D_k is a sequence of data bits of amplitude (± 1) and duration T_b seconds, and $b_k(t - kT_b)$ is the PN sequence pattern for the k^{th} bit, i.e.,

$$b_k(t) = \sum_{j=1}^L c_{kj} q(t - jT_c) \quad (4)$$

with L being the number of pseudo random chips per bit, or the processing gain, c_{kj} is the code sequence for the bit, and $q(t)$ represents the basic chip pulse of energy E_c .

The noise $n(t)$ is Gaussian and has a power spectral density

$$S_n(f) = \frac{N_0}{2} |H_{bp}(f)|^2, \quad (5)$$

where $N_0/2$ is the power spectral density of the assumed white Gaussian noise from the channel. The band of interference is defined as

$$i(t) = I(t) \cos(\omega_0 t + \theta(t)) \quad (6)$$

where $I(t)$ is the interference amplitude and $\theta(t)$ is the phase modulation. It has been assumed that the effect of the bandpass filter $H_{bp}(f)$ is negligible on the interference $i(t)$.

Referring to Fig. 1, the output $u(t)$ of the bandpass filter $H_{bp}(f)$ is bandpass sampled and applied to a limiter/bandpass filter and interference estimator.

Consider the bandpass sampler first. The analog signal $u(t)$ from Eq. (1) is

sampled at $f_s = 2R_c$ ($mf_s = \omega_0/2\pi + R_c/2$ for some integer m) where R_c is the chip rate of the spread spectrum signal. The resultant sampled signal is, therefore,

$$u_n = s_n + n_n + i_n, \quad (7)$$

where s_n consists of the sequence $\{\dots, 0, (-1)^n a_n, 0, (-1)^{n+2} a_{n+2}, \dots\}$ where the a_n are of energy E_c and coded according to c_k, D_k for the j^{th} chip in the k^{th} transmitted bit. n_n ¹ are uncorrelated Gaussian noise samples of variance $\sigma_{nse}^2 = E_c(N_0/2)$, and i_n is the sampled version of Eq. (6). The samples u_n are applied to the interference estimator and interference canceller.

The interference estimator produces an estimate \hat{i}_n of the interference which is removed from the sampled input u_n . The output of the summer is decimated and sign-reversed, resulting in a baseband error signal e_n . This error signal is correlated with the PN sequence. The output of the correlator is integrated and bit-detected.

Consider now the branch containing the limiter. Here, u_n is applied to a limiter/bandpass filter. The input to the limiter referenced to the interference is redefined as

$$u_n = \sqrt{[I_n + n'_{1,n} + a'_{1,n}]^2 + [n'_{2,n} + a'_{2,n}]^2} \cos[\omega_0 n + \theta_n + \phi_{u,n}] \quad (8)$$

where

$$\phi_{u,n} = \arctan \left(\frac{n'_{2,n}/\sqrt{2} + a'_{2,n}}{I_n + n'_{1,n}/\sqrt{2} + a'_{1,n}} \right) \quad (9)$$

is a noise-like phase fluctuation on the interferer's phase θ_n , and is due to the noise and spread spectrum signal. The terms $n'_{1,n}$, $n'_{2,n}$, $a'_{1,n}$, and $a'_{2,n}$ are in-phase and quadrature components of the noise and spread spectrum signal with respect to the interference phase θ_n .

The output of the limiter/bandpass filter is [4]

$$bp_n = \frac{4A'}{\pi} \cos[\omega_0 n + \theta_n + \phi_{u,n}], \quad (10)$$

where A' is the limiter's output level. This signal is redefined as (letting $A' = \sqrt{2}\pi/4$ for convenience)

$$bp_n = \sqrt{2} \cos[\omega_0 n + \theta_n + \phi_{u,n}]. \quad (11)$$

It should be noted that for large interference-to-noise ratios in which the interference is

¹Coherent bandpass sampling has been assumed, so that the in-phase component is $(n_{1,n}/\sqrt{2}) \cos(n\pi/2)$ and the quadrature component is $(n_{2,n}/\sqrt{2}) \sin(n\pi/2)$

of constant envelope, $\phi_{u,n}$ in Eq. (11) is approximately Gaussian [4]. The sampled signal in Eq. (11) is what is processed by the Kalman filter, which estimates the phase θ_n of the interference. The phase estimate is denoted as $\hat{\theta}_{n|n-1}$

3.0 INTERFERENCE ESTIMATOR

The interference estimator shown in Fig. 1 is detailed in Fig. 2. The Kalman algorithm [3] produces a signal

$$\hat{y}_n = \sqrt{2} \cos(\omega_0 n + \hat{\theta}_{n|n-1}) \quad (12)$$

which can be used as a basis for estimating a sampled version of the envelope of $i(t)$ (i.e., I_n in Eq. (6)). The output of the first multiplier is a baseband term and is, using Eq. (7), excluding the $\sqrt{2}$ factor,

$$\begin{aligned} \hat{I}'_n &= I_n \cos(\theta_n - \hat{\theta}_{n|n-1}) \\ &+ n_n \cos(\omega_0 n + \hat{\theta}_{n|n-1}) + a_n \cos(\hat{\theta}_{n|n-1}) \\ &+ a_n \cos(2\omega_0 n + \hat{\theta}_{n|n-1}) \end{aligned} \quad (13)$$

Equation (13) consists of four terms: the first term is related to the desired envelope of

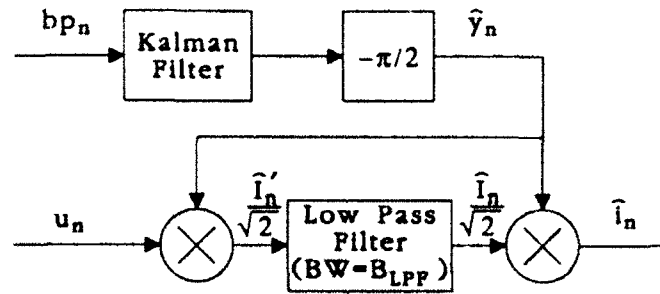


Figure 2: Block diagram of the interference estimator.

the interference; the second is approximately Gaussian baseband noise [5]; and the third and fourth terms are noise-like terms emanating from the spread spectrum signal. The fourth term, because of the sampling rate conditions discussed in [6], is essentially filtered out by the low pass filter of bandwidth $B_{LPP} < 0.50$ Hz and, therefore, will be ignored in the baseband simulations to be discussed in the next section. The term $\hat{I}'_n / \sqrt{2}$ is filtered, resulting in the estimate of the interference envelope, $\hat{I}_n / \sqrt{2}$. Combining this with \hat{y}_n in Eq. (12) and shown in Fig. 2, yields the estimate of the interference

$$\hat{i}_n = \hat{I}_n \cos(\omega_0 n + \hat{\theta}_{n|n-1}), \quad (14)$$

which is subtracted from u_n as illustrated in Fig. 1.

4.0 NARROWBAND GAUSSIAN NOISE INTERFERENCE

The interference that is considered is narrowband Gaussian noise. In [1, 2], the envelope was constant. For narrowband Gaussian noise, the envelope varies as well as the phase. There are two issues to be concerned with here that are related to the time-varying envelope. First, the low pass filter used in estimating the envelope I_n in Fig. 2 will introduce a lag in \hat{I}_n thereby increasing the amount of residual interference at the output of the canceller. Second, a time-varying envelope will have the impact of introducing larger phase errors, particularly when the envelope gets very small, since the Kalman filter will not be able to track the fast phase transitions during these instances. These effects will now be dealt with at length.

4.1 FILTER LAG EFFECTS

First consider the effect of the lag introduced by the Butterworth filter of bandwidth B_{LPF} in estimating I_n in Fig. 2. The effect can be observed if one graphs the degree of interference suppression at the output of the excisor as a function of d , the frequency deviation constant of the Kalman filter, for a particular interference bandwidth B_i for several values of B_{LPF} . Interference suppression is defined in [1] as

$$S = 10 \log(\overline{\Delta i_n^2} / P_i) \quad (15)$$

where $\Delta i_n = i_n - \hat{i}_n$ is the residual interference, and P_i is the power in the interference. As an example, Fig. 3 illustrates the degree of interference suppression as a function of d , when the interference bandwidth is $B_i = 0.02$ Hz. The interference was generated by applying white Gaussian noise to a fourth order lowpass Butterworth filter resulting in the baseband interference $i_n = I_n \cos(\theta_n)$. Observe that as B_{LPF} increases, the degree of suppression improves. This phenomenon is due to the reduction in the lag as B_{LPF} increases. It is more clearly illustrated in Figs. 4 and 6, in which sections of the envelope I_n and its estimate \hat{I}_n have been plotted for $B_{LPF} = 0.20$ and 0.40 Hz for the case when $d = 0.30$ rad./sec/volt which is approximately the minimum in Fig. 3. A comparison of Fig. 6 with Fig. 4 reveals a reduction in the delay but, as to be expected, an increase in envelope noise. The effect of the delay is further illustrated in Figs. 5 and 7 for the overall interference i_n and \hat{i}_n for the two cases. In Fig. 5, one can also see the effect of the phase-noise, since the envelope noise for this case was small as indicated in Fig. 4.

From these results, and the results of [1, 2] concerning constant envelope interference, there are conflicting requirements. The results from the constant envelope analysis suggested the use of as small a bandwidth for the lowpass filter as possible, whereas here, as large a value as possible is required to reduce the lag, but at the expense of introducing more envelope noise and signal distortion. This suggests that one could compensate for the delay or use a linear phase FIR filter with some predefined delay. Either of these approaches will, of course, translate into the requirement for a similar delay in the PN correlator. The remainder of this technical note will consider an FIR low pass filter with pre-defined delay.

To accomodate this change, the interference estimator of Fig. 2 will have to be modified somewhat to account for this type of filter. The modified version of Fig. 2 is illustrated in Fig. 8. The FIR low pass filter has a delay D , which requires that \hat{y}_n in Fig. 2 and Eq. 12 must be delayed by D as well to yield

$$\hat{y}_{n-D} = \sqrt{2} \cos[\omega_0(n-D) + \hat{\theta}_{n-D}] \quad (16)$$

before combining it with the envelope estimate, \hat{I}_{n-D} , to produce the interference estimate \hat{i}_{n-D} . This requires too that the input signal $u_n = s_n + n_n + i_n$ be delayed by D samples before removal of the interference estimate. The output of the canceller is

$$\begin{aligned} e_{n-D} &= u_{n-D} - \hat{i}_{n-D} \\ &= s_{n-D} + n_{n-D} + i_{n-D} - \hat{i}_{n-D}. \end{aligned} \quad (17)$$

This error signal is then applied to the PN correlator whose PN sequence is delayed by D as well.

A comparison of the suppression performance of the systems in Figs. 2 and 8 is now presented.

The bandwidth of the FIR and Butterworth filters for this case was $B_{LPF} = 0.20$ Hz. The FIR filter had 7 taps with rectangular weighting, the interference bandwidth was $B_i = 0.02$ Hz and $E_b/N_0 = 12$ dB. The results are illustrated in Fig. 9 and indicate that the FIR filter improves the amount of interference suppression by 2.7 dB. Furthermore, a comparison of Fig. 3 with Fig. 9 shows that the FIR filter of bandwidth 0.20 Hz provides an additional 1 dB of interference suppression over the Butterworth filter of bandwidth 0.40 Hz. This gives one some idea of the degradation in performance produced by the additive envelope noise using the interference estimator in Fig. 2 for the larger bandwidth situation.

Examples of the envelope and interference estimates are also illustrated in Figs. 10

and 11. Notice in Fig. 11 between 200 and 300 seconds the additional noise due to phase-noise. Finally, Fig. 12 shows the suppression level for several interference bandwidths, with $B_{LPF} = 0.20$ Hz and $E_b/N_0 = 12$ dB. It is important to note here that as the bandwidth of the interference increases, the value of d at which the minimum occurs increases, emphasizing the requirement for a larger Kalman filter bandwidth, which is controlled by d (everything else being constant), to cope with the faster rate of change of the phase.

4.2 PHASE-NOISE EFFECTS

The second issue to consider is the tendency of the Kalman filter to temporarily lose track when the phase varies rapidly during those instances when the envelope becomes small. It is conceivable, therefore, that with some additional phase-smoothing apart from that provided by the Kalman filter, the phase estimates can improve, thereby reducing envelope and phase-noise caused by inaccurate phase estimates.

To accomodate this idea, an additional modification must be made to the interference estimator in Fig. 8; this change is illustrated in Fig. 13. In this figure, the phase estimate $\hat{\theta}_{n|n-1}$ from the Kalman filter in Fig. 4 of [3] is applied to a simple N -point smoother implemented as an FIR comb filter that introduces the same delay D as the FIR filter used in filtering the envelope. The result is the smoothed phase $\hat{\theta}'_{n-D}$ which is applied to a phase modulator, yielding the signal

$$\hat{y}'_{n-D} = \sqrt{2} \cos[\omega_0(n-D) + \hat{\theta}'_{n-D}]. \quad (18)$$

This signal is combined with the envelope estimate \hat{I}_{n-D} to produce the interference estimate

$$\hat{i}_{n-D} = \hat{I}_{n-D} \cos[\omega_0(n-D) + \hat{\theta}'_{n-D}] \quad (19)$$

that is then subtracted from the delayed input u_{n-D} to yield the error signal e_{n-D} .

Figure 14 shows a section of the phase θ_n and its Kalman filtered estimate $\hat{\theta}_{n|n-1}$ for the case when the interference bandwidth is $B_i = 0.02$ Hz and $d = 0.30$ rad./sec./volt using the system in Fig. 8. This should be compared with Fig. 15, which is a 7-point smoothed version of $\hat{\theta}_{n|n-1}$ based on the system in Fig. 13; the effect of smoothing the phase estimate is quite apparent. Figure 16 shows a magnified version of a segment of interference i_n along with the estimates obtained with and without phase smoothing. Here too, the improvement is quite noticeable.

The level of interference suppression as a function of d is illustrated in Fig. 17 for several interference bandwidths. As can be seen, the degree of suppression has improved by 3 to 4 dB in comparison with the results in Fig. 12 in which no phase-smoothing

was used. In addition, there is a broader range of values for d over which the maximum suppression level can be maintained.

The bit error rate performance of the two interference estimators in Figs. 8 and 13 is presented next as determined from computer simulation. The test conditions were as follows. A total of 50,000 bits were transmitted with a processing gain of $L = 20$, implying a total of 1,000,000 chips. The interference was narrowband Gaussian noise ranging in bandwidth from $B_i = 0.01$ Hz to 0.05 Hz. The approximated optimum values for d obtained from Figs. 12 and 17 were used in the Kalman filter. The term α_f was set at 0.0003125 Hz and the spectral density of the observation noise $N_{obs}/2$ was obtained from Eq. (23) of [1], with I^2 replaced by \bar{I}_n^2 , the mean-squared value of the envelope. The bandwidth, B_{LPF} , selected for the linear phase FIR filter was 0.20 Hz and introduced a delay of $D = 3$ samples. The phase estimate $\hat{\theta}_{n|n-1}$ in Fig. 13 was applied to a 7-point rectangular smoother, which also introduced a delay of $D = 3$ samples.

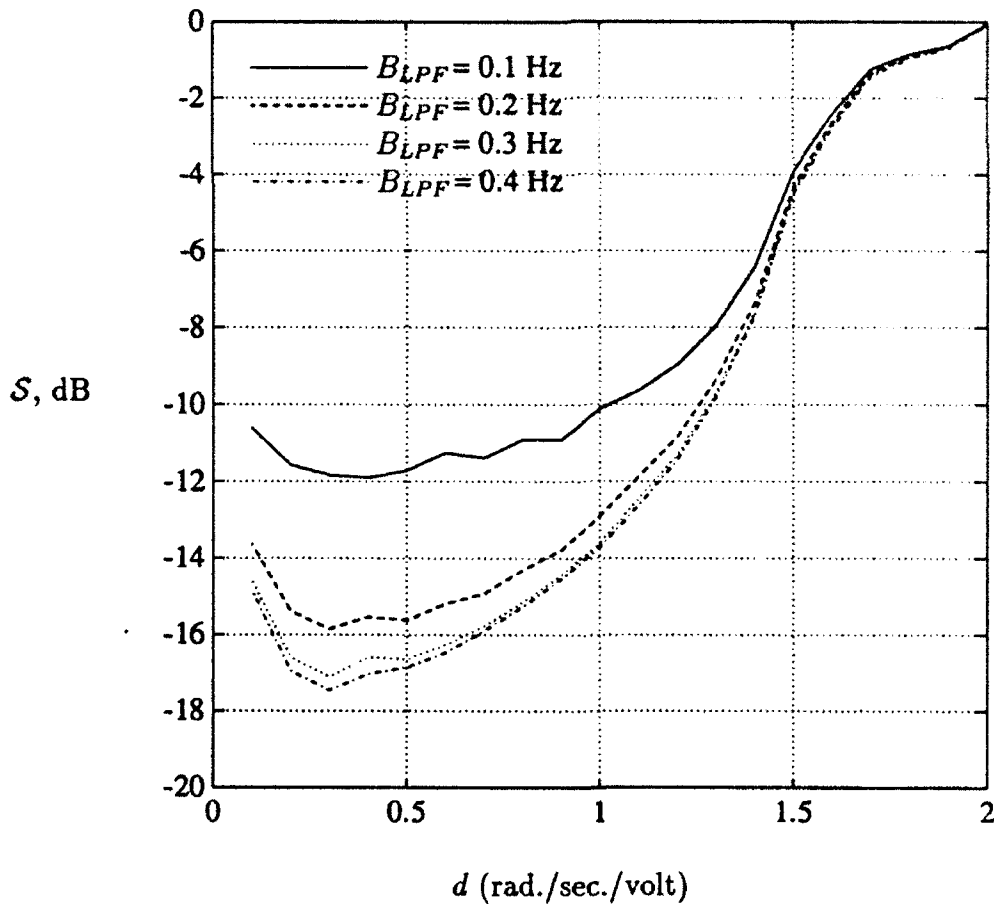


Figure 3: Level of interference suppression S as a function of d for several lowpass filter bandwidths. The interference is narrowband Gaussian noise of bandwidth 0.02 Hz.

The results of the two interference estimators are plotted in Figs. 18 and 19. The bit error rate performance of the interference estimator with phase-smoothing (Fig. 19) indicates a significant improvement in performance over its non-smoothed counterpart shown in Fig. 18. In fact, the improvement is 4 to 5 dB in each of the cases when bit error rates at $E_b/N_0 = 12$ dB are compared. These results also indicate the role of the phase-noise in so far as its effect on the bit error rate for narrowband Gaussian noise is concerned. This was also exhibited in the amount of interference suppression between the two approaches (Figs. 12 and 17). There too the improvement in suppression was approximately 4 dB.

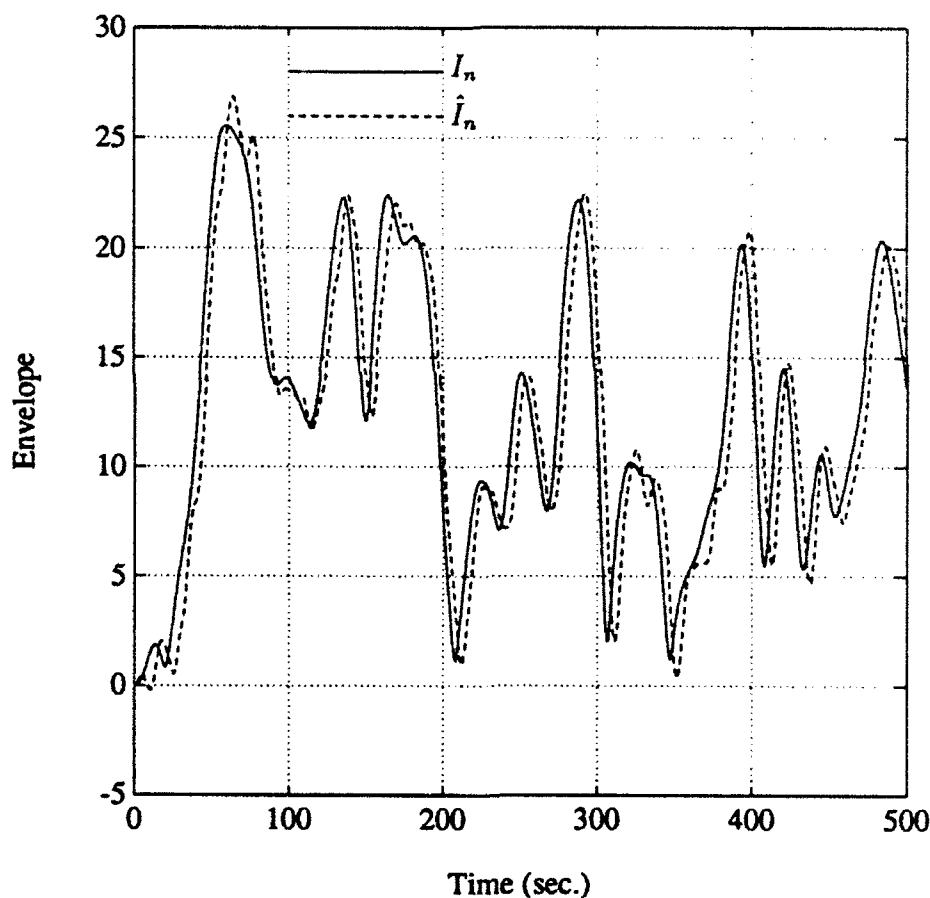


Figure 4: An example of a portion of the envelope I_n and its estimate \hat{I}_n when the filter is of the Butterworth type of bandwidth $B_{LPF} = 0.20$ Hz with $d = 0.30$ rad./sec./volt and interference bandwidth $B_i = 0.02$ Hz.

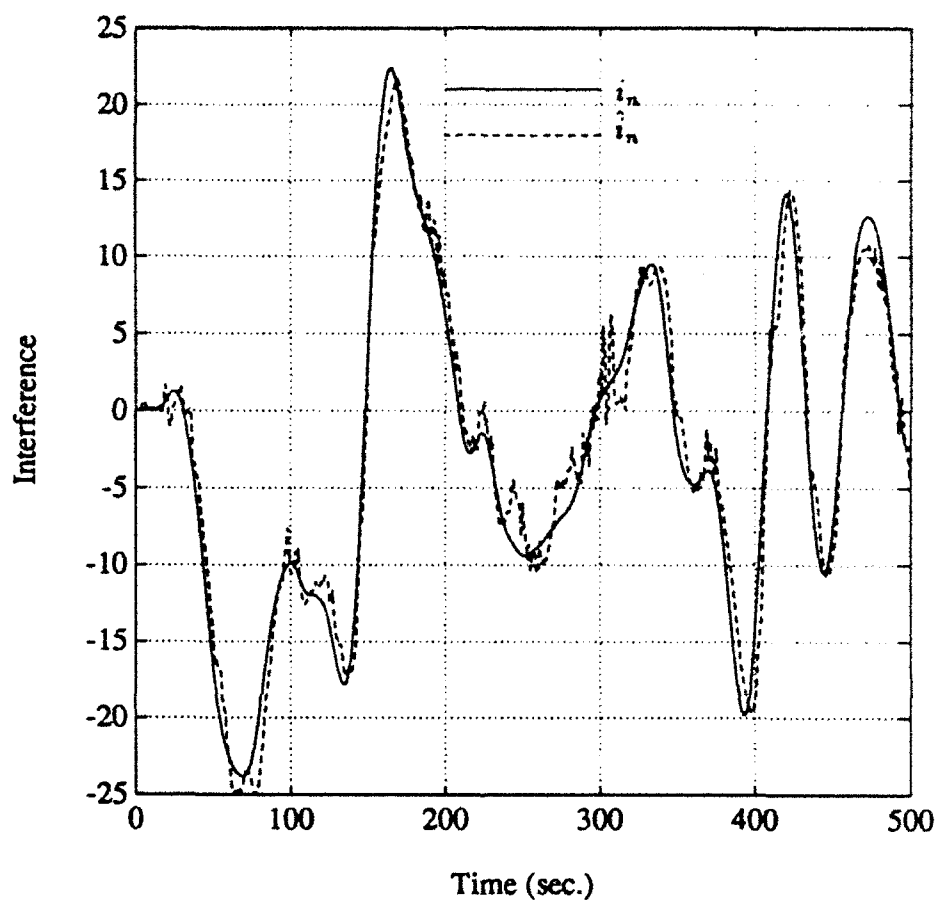


Figure 5: An example of a portion of the interference i_n and its estimate \hat{i}_n when the filter is of the Butterworth type of bandwidth $B_{LPF} = 0.20$ Hz, $d = 0.30$ rad./sec./volt and interference bandwidth $B_i = 0.02$ Hz.

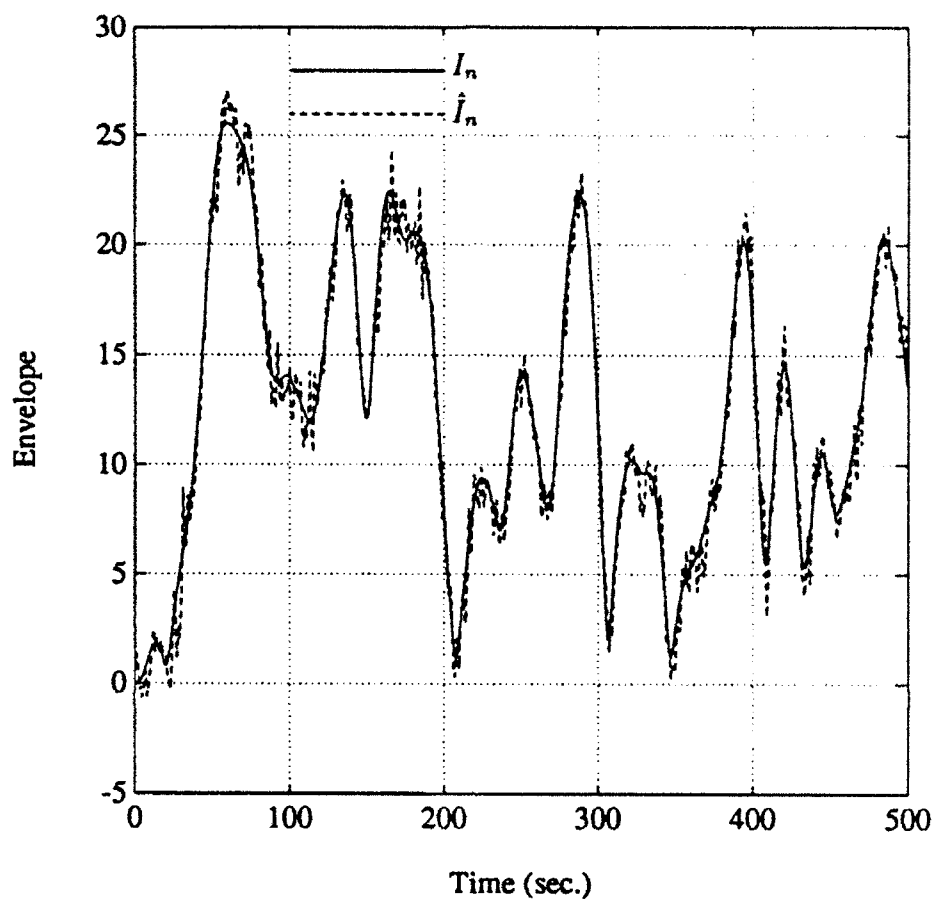


Figure 6: An example of a portion of the envelope I_n and its estimate \hat{I}_n when the filter is of the Butterworth type of bandwidth $B_{LPF} = 0.40$ Hz with $d = 0.30$ rad./sec./volt and interference bandwidth $B_i = 0.02$ Hz.

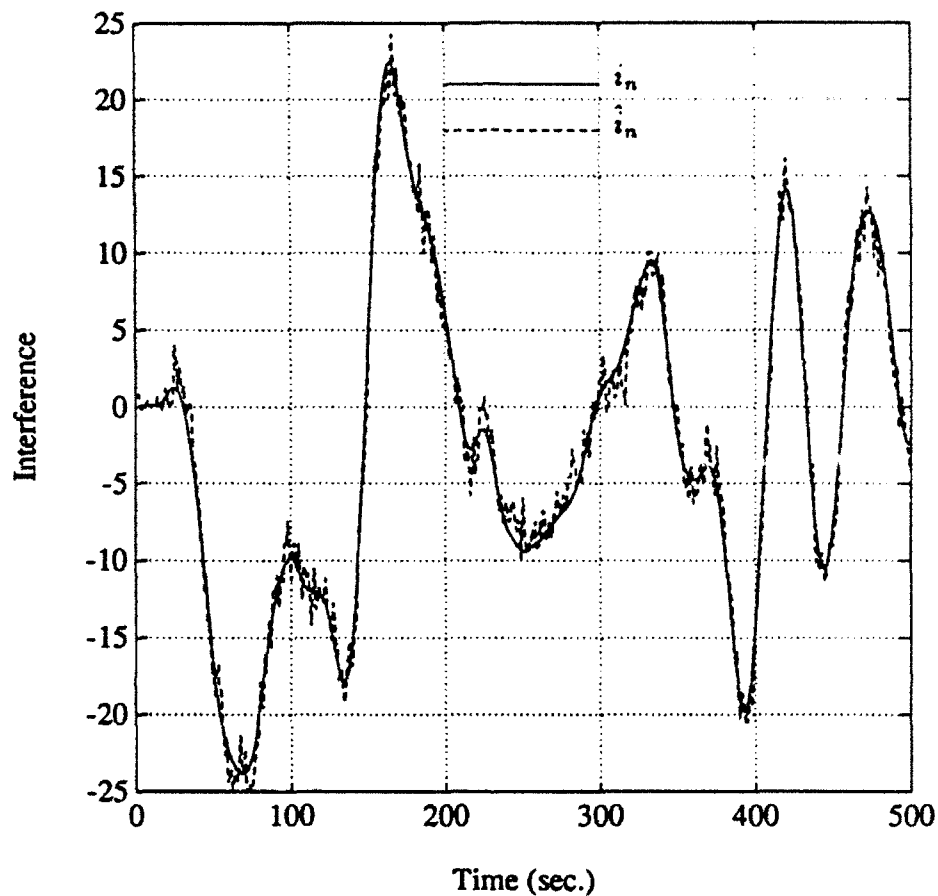


Figure 7: An example of a portion of the interference i_n and its estimate \hat{i}_n when the filter is of the Butterworth type of bandwidth $B_{LPF} = 0.40$ Hz, $d = 0.30$ rad./sec./volt and interference bandwidth $B_i = 0.02$ Hz.

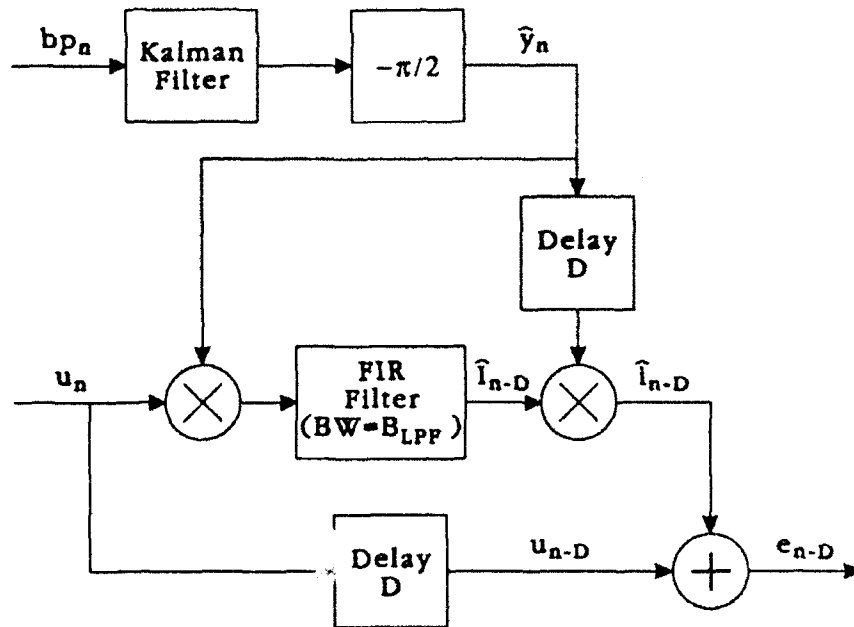


Figure 8: Modified interference estimator of Fig. 2 when the low pass filter is a linear phase FIR filter.

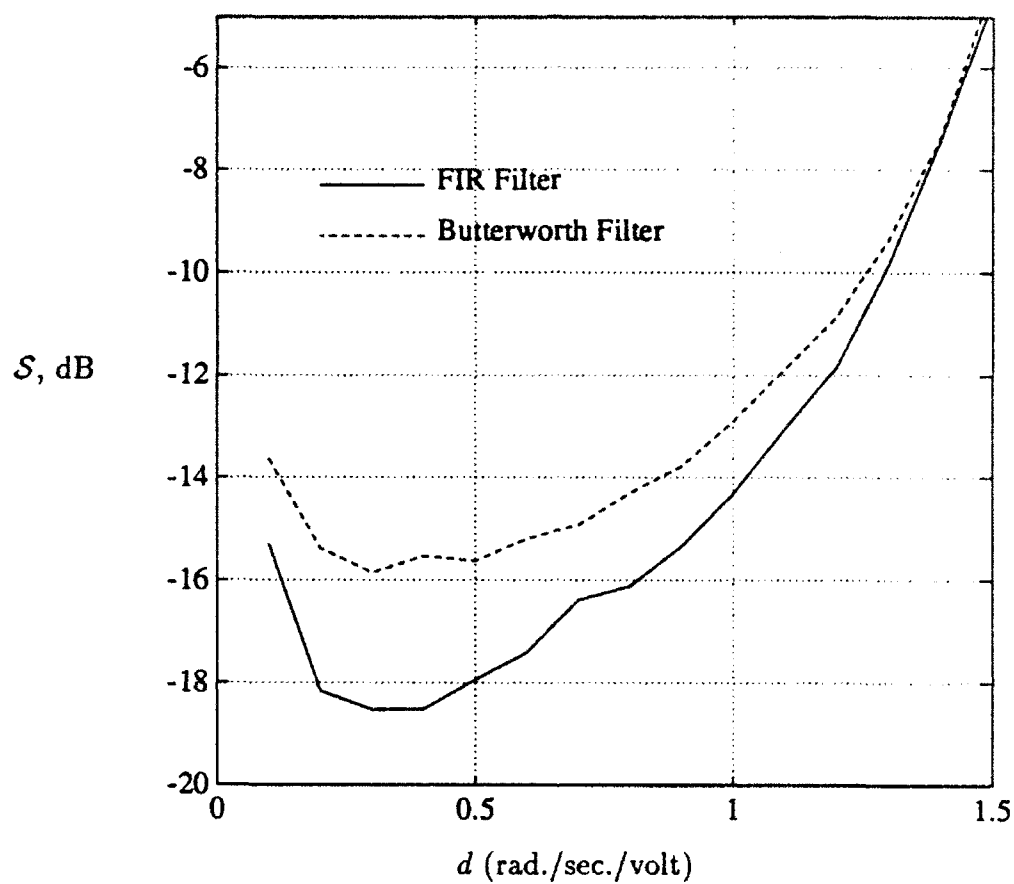


Figure 9: Comparison of the interference suppression levels S produced by a 7-tap FIR filter and 4th order Butterworth filter when $B_i = 0.02$ Hz, $B_{LPF} = 0.20$ Hz, and $E_b/N_0 = 12$ dB.

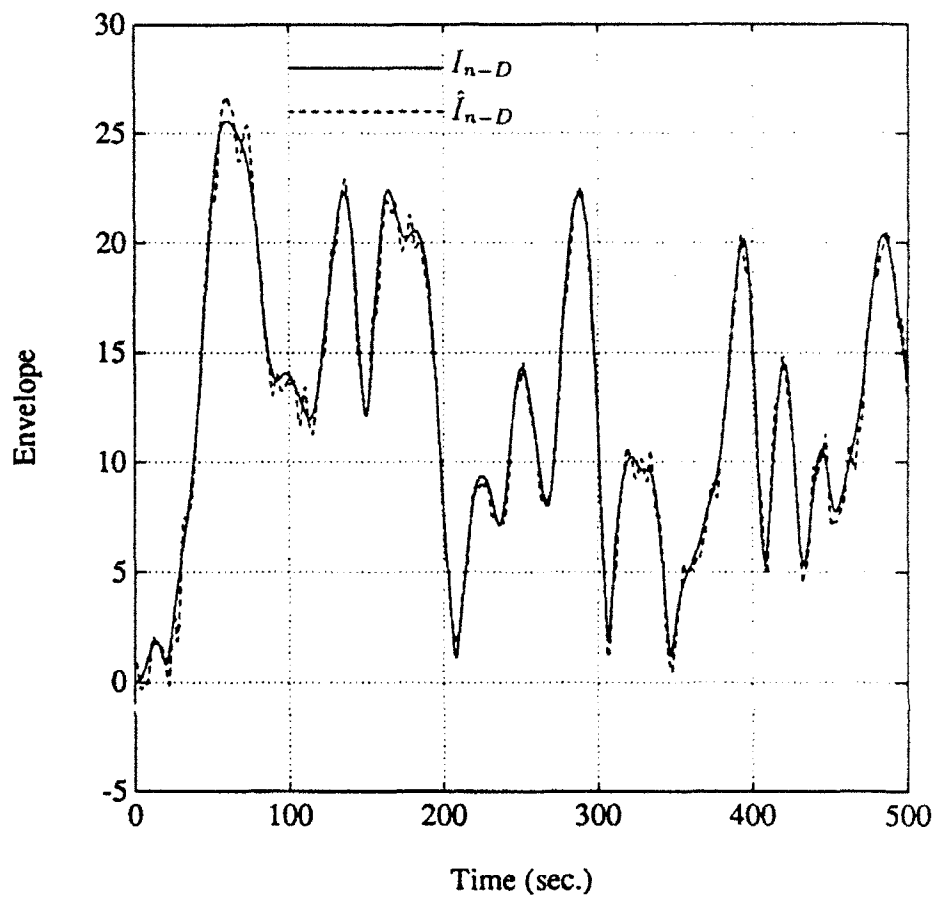


Figure 10: An example of a portion of the envelope I_{n-D} and its estimate \hat{I}_{n-D} when the filter is of the linear phase FIR type of bandwidth $B_{L,PF} = 0.20$ Hz with $d = 0.30$ rad./sec./volt and interference bandwidth $B_i = 0.02$ Hz.

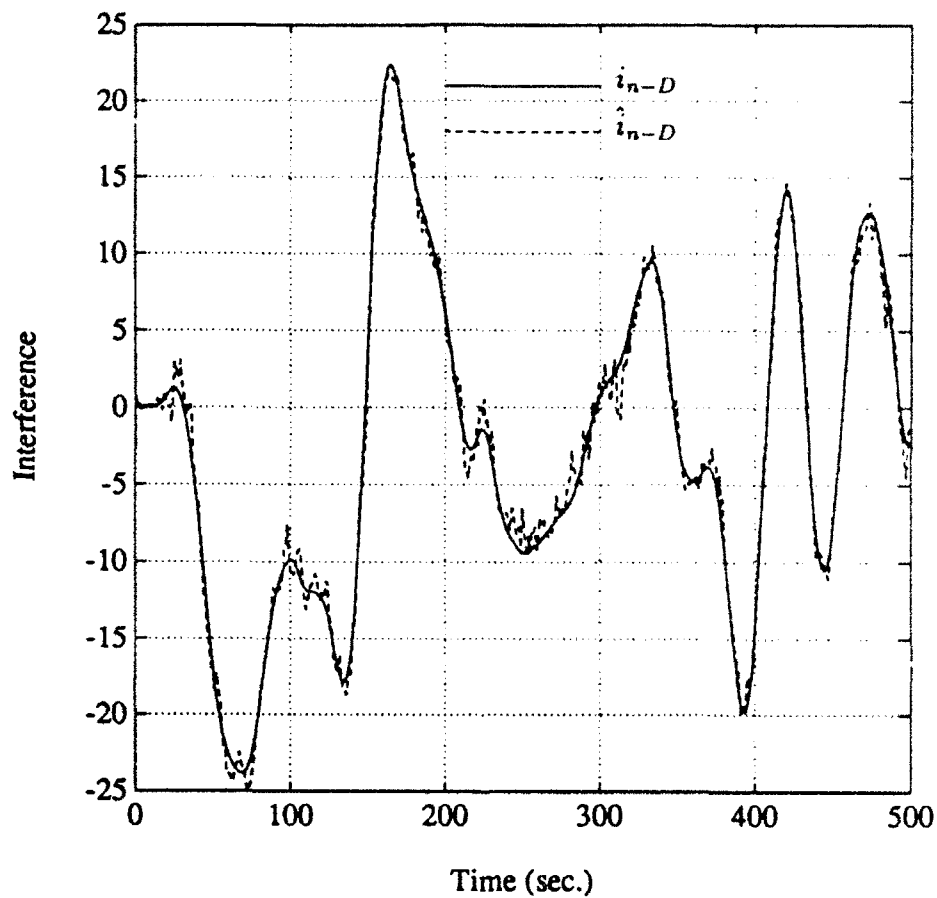


Figure 11: An example of a portion of the interference i_{n-D} and its estimate \hat{i}_{n-D} when the filter is of the FIR type of bandwidth $B_{LPF} = 0.20$ Hz, $d = 0.30$ rad./sec./volt and interference bandwidth $B_i = 0.02$ Hz.

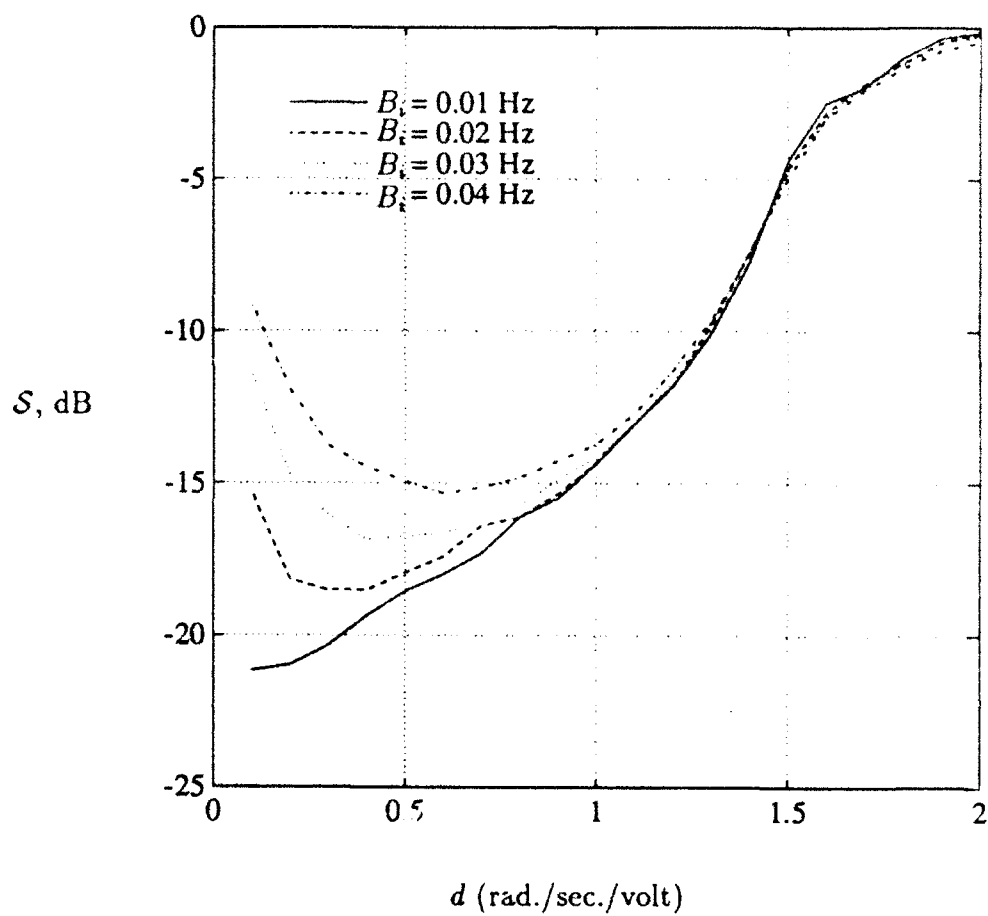


Figure 12: Interference suppression level S as a function of d for several interference bandwidths, B_i , ranging from 0.01 Hz to 0.04 Hz, with $B_{LPF} = 0.20$ Hz.

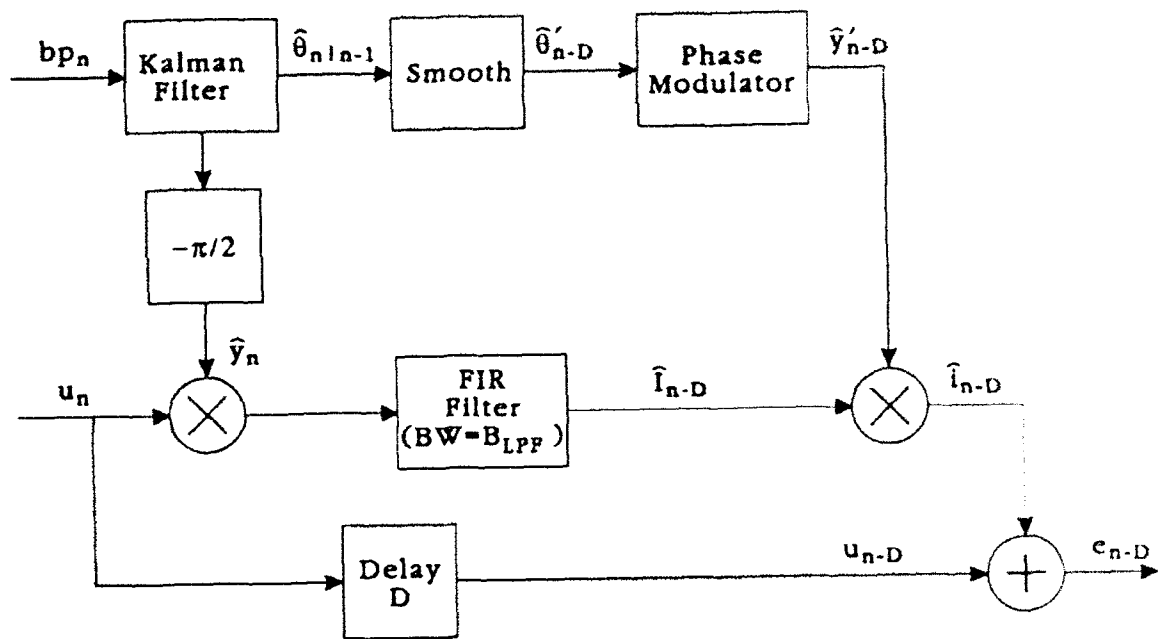


Figure 13: Interference estimator when phase-smoothing is being used.

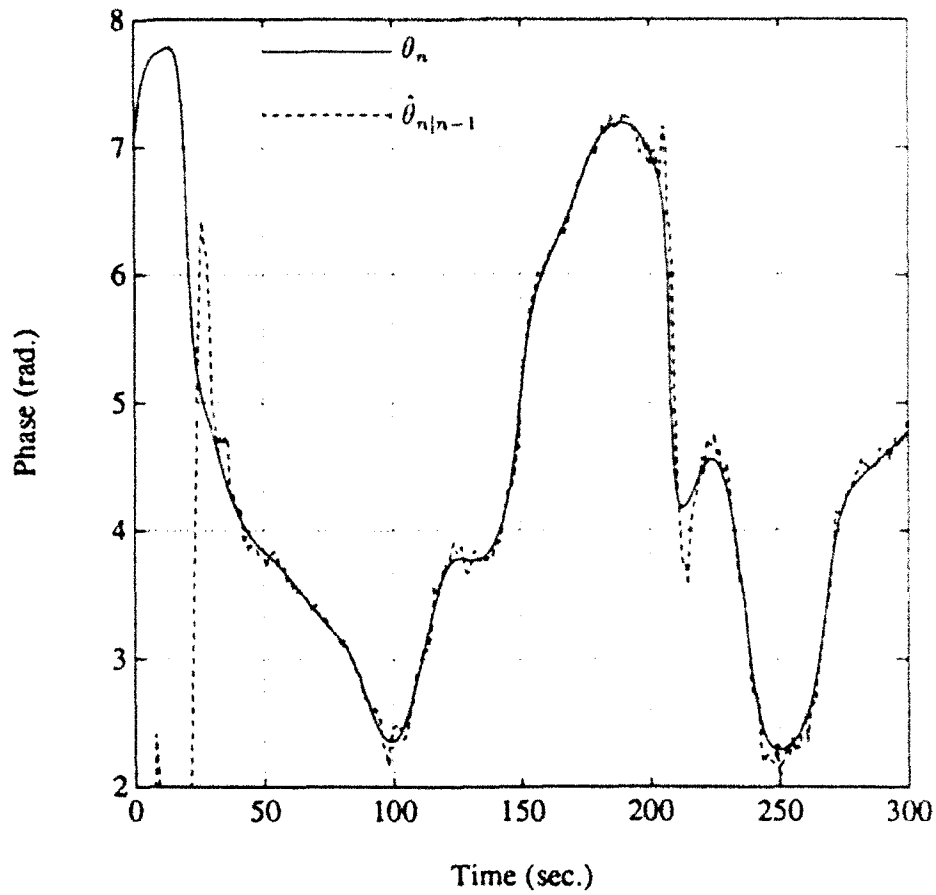


Figure 14: An example of the phase θ_n and its Kalman filter estimate $\hat{\theta}_{n|n-1}$, with interference bandwidth $B_i = 0.02$ Hz and $d = 0.30$ rad./sec./volt.

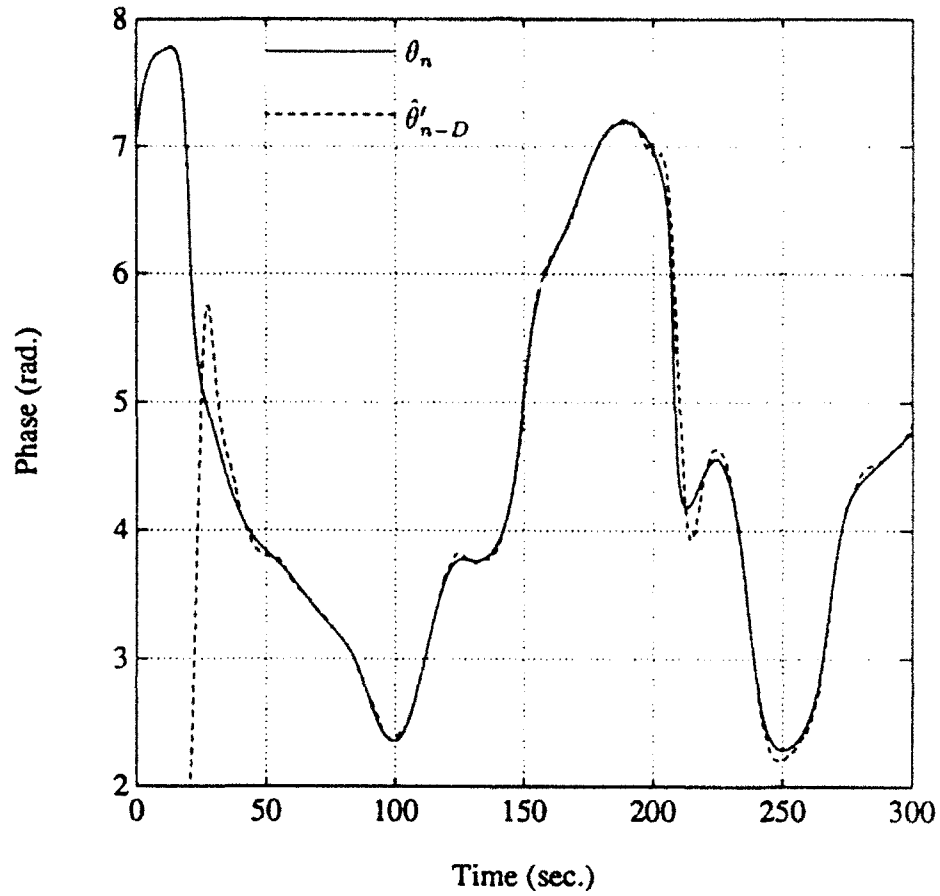


Figure 15: An example of the phase θ_n and a 7-point smoothed version $\hat{\theta}'_{n-D}$ of its Kalman filter estimate $\hat{\theta}_{n|n-1}$, with interference bandwidth $B_i = 0.02$ Hz and $d = 0.30$ rad./sec./volt.

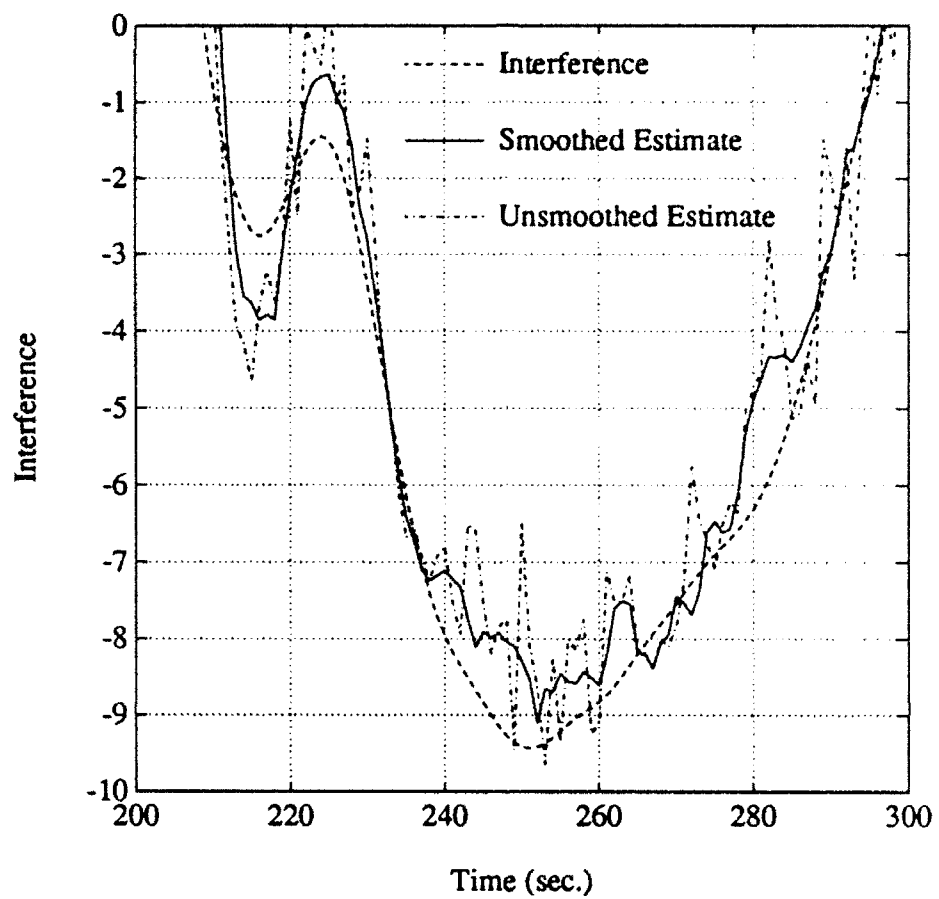


Figure 16: An example of a segment of interference with and without phase smoothing; interference bandwidth $B_i = 0.02$ Hz and $d = 0.30$ rad./sec./volt.

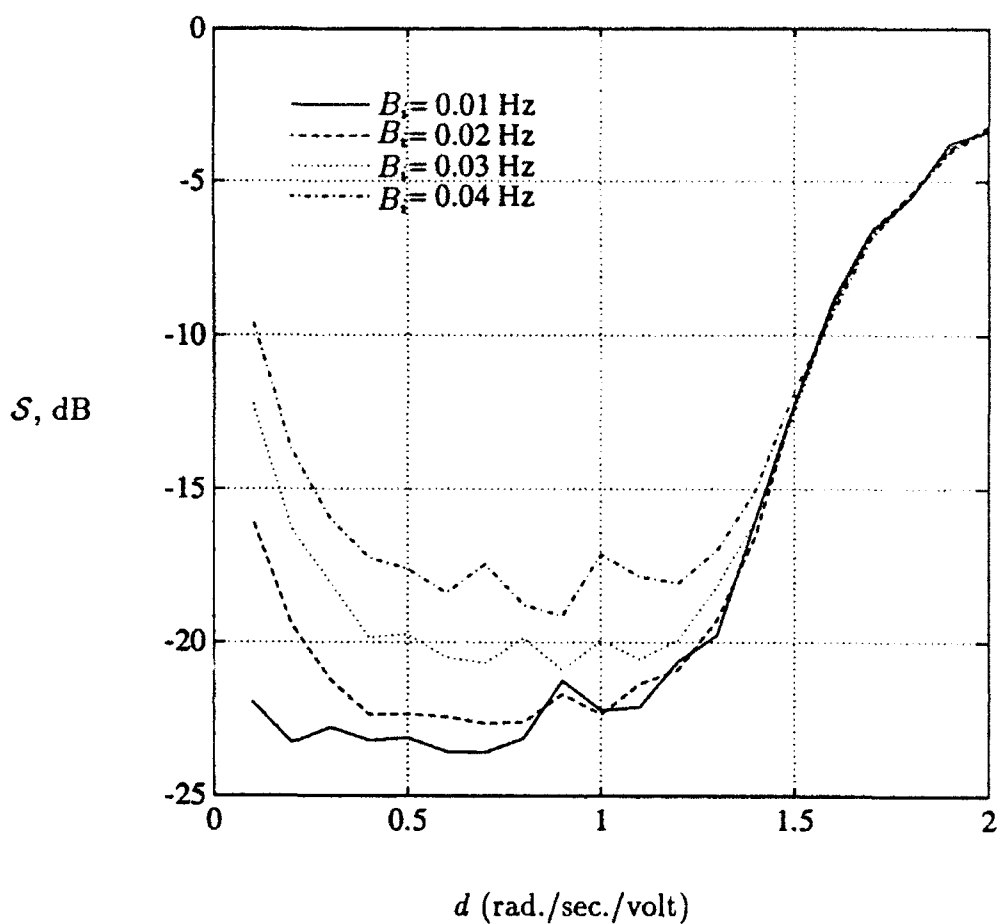


Figure 17: Interference suppression level S as a function d for several interference bandwidths, B_i , ranging from 0.01 Hz to 0.05 Hz, with $B_{LPF} = 0.20$ Hz.

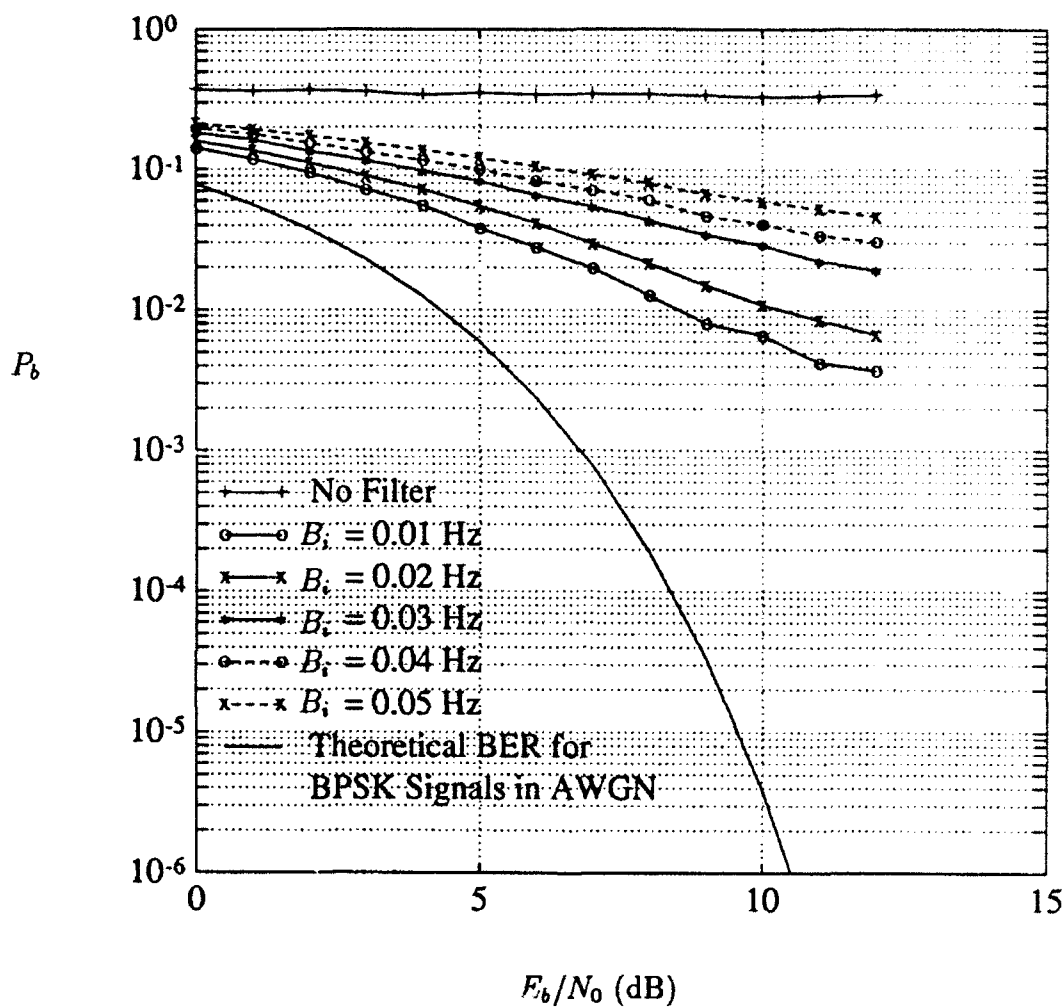


Figure 18: Bit error rate for the case of narrowband Gaussian noise with bandwidths B_i ranging from 0.01 Hz to 0.05 Hz, using the optimum values of d obtained from Fig. 17, and an FIR filter with no averaging on the phase estimate $\hat{\theta}_{n|n-1}$.

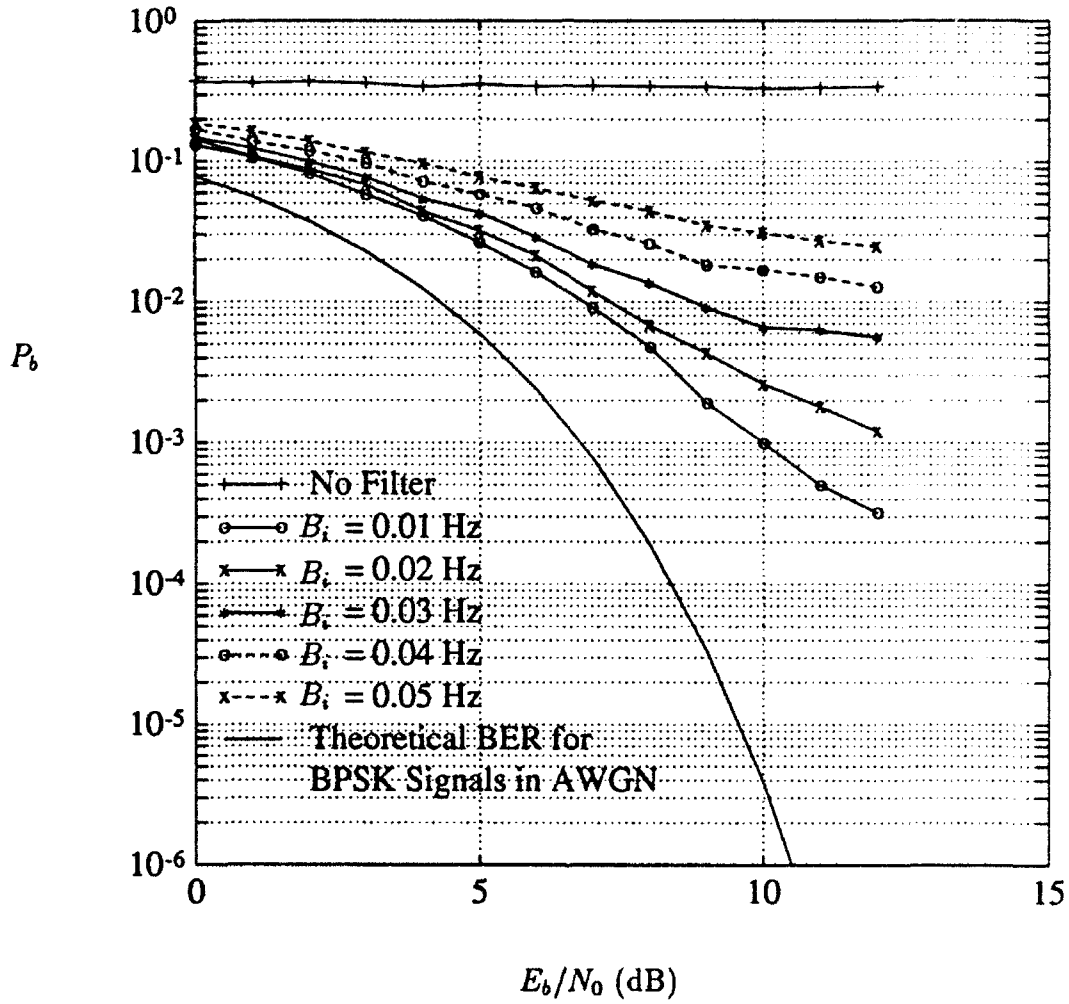


Figure 19: Bit error rate for the case of narrowband Gaussian noise with bandwidths B_i ranging from 0.01 Hz to 0.05 Hz, using the optimum values of d obtained from Fig. 17, and an FIR filter with 7-point averaging on the phase estimate $\hat{\theta}_{n|n-1}$.

5.0 CONCLUSIONS

This technical note has presented an improved Kalman filtering excisor to deal with the more general type of interference—narrowband Gaussian noise, which would be representative of the case when, say, several independent, narrowband interferers are lumped close together in some region of the frequency band also occupied by the direct sequence spread spectrum signal. Under these conditions, both the envelope and phase of the composite interference will vary, resulting in poorer performance of the basic Kalman filter excisor described in earlier reports.

This technical note presented the essence of the problem in so far as the Kalman filter is concerned when narrowband Gaussian interference is present. Two enhancements were suggested and evaluated. It was shown that up to 5 dB of improvement could be attained with the revised excisor.

It should be noted that only one value of low pass filter bandwidth B_{LPF} (i.e., 0.20 Hz) was selected for these comparisons, and only one type of phase-smoother. Other combinations may produce superior performance; however, further work would have to be conducted to assess if indeed this would be possible. Finally, given the significance of the phase-noise at the output of the Kalman filter for narrowband Gaussian noise interference, other architectures perhaps can be developed using the phase-smoothing concept to further improve performance.

REFERENCES

- [1] B. W. Kozminchuk, "A comparison of recursive least squares and Kalman filtering excisors for swept tone interference," Technical Note 92-14, Defence Research Establishment Ottawa, Ottawa, Ontario, Canada, K1A 0Z4, 1992.
- [2] B. W. Kozminchuk, "Theoretical bit error rate performance of the Kalman filter excisor for FM interference," Technical Report To be published, Defence Research Establishment Ottawa, Ottawa, Ontario, Canada, K1A 0Z4, 1992.
- [3] B. W. Kozminchuk, "Kalman filter-based architectures for interference excision," Technical Report 1118, Defence Research Establishment Ottawa, Ottawa, Ontario, Canada, K1A 0Z4, 1991.
- [4] A. Blanchard, *Phase-Locked Loops*. New York: John Wiley and Sons, 1976.
- [5] H. L. Van Trees, *Detection, Estimation, and Modulation-Part 2: Nonlinear Modulation Theory*. New York: John Wiley and Sons, 1971.
- [6] D. R. Polk and S. C. Gupta, "Quasi-optimum digital phase-locked loops," *IEEE Transactions on Communications*, vol. 21, pp. 75-82, January 1973.

SECURITY CLASSIFICATION OF FORM
(highest classification of Title, Abstract, Keywords)

DOCUMENT CONTROL DATA

(Security classification of title, body of abstract and indexing annotation must be entered when the overall document is classified)

1. ORIGINATOR (the name and address of the organization preparing the document. Organizations for whom the document was prepared, e.g. Establishment sponsoring a contractor's report, or tasking agency, are entered in section 8.) DEFENCE RESEARCH ESTABLISHMENT OTTAWA DEPARTMENT OF NATIONAL DEFENCE SHIRLEY BAY, OTTAWA, ONTARIO K1A 0K2 CANADA		2. SECURITY CLASSIFICATION (overall security classification of the document including special warning terms if applicable) <p align="center">UNCLASSIFIED</p>	
3. TITLE (the complete document title as indicated on the title page. Its classification should be indicated by the appropriate abbreviation (S.C or U) in parentheses after the title.) AN IMPROVED KALMAN FILTER EXCISOR FOR SUPPRESSING NARROWBAND GAUSSIAN NOISE INTERFERENCE (U)			
4. AUTHORS (Last name, first name, middle initial) KOZMINCHUK, BRIAN W.			
5. DATE OF PUBLICATION (month and year of publication of document) NOVEMBER 1992		6a. NO. OF PAGES (total containing information. Include Annexes, Appendices, etc.) 34	6b. NO. OF REFS (total cited in document) 6
7. DESCRIPTIVE NOTES (the category of the document, e.g. technical report, technical note or memorandum. If appropriate, enter the type of report, e.g. interim, progress, summary, annual or final. Give the inclusive dates when a specific reporting period is covered.) DREO TECHNICAL NOTE			
8. SPONSORING ACTIVITY (the name of the department project office or laboratory sponsoring the research and development. Include the address.) DEFENCE RESEARCH ESTABLISHMENT OTTAWA DEPARTMENT OF NATIONAL DEFENCE SHIRLEY BAY, OTTAWA, ONTARIO K1A 0K2 CANADA			
9a. PROJECT OR GRANT NO. (if appropriate, the applicable research and development project or grant number under which the document was written. Please specify whether project or grant) 041LK11		9b. CONTRACT NO. (if appropriate, the applicable number under which the document was written)	
10a. ORIGINATOR'S DOCUMENT NUMBER (the official document number by which the document is identified by the originating activity. This number must be unique to this document.) DREO TECHNICAL NOTE 92-28		10b. OTHER DOCUMENT NOS. (Any other numbers which may be assigned this document either by the originator or by the sponsor)	
11. DOCUMENT AVAILABILITY (any limitations on further dissemination of the document, other than those imposed by security classification) <input checked="" type="checkbox"/> Unlimited distribution <input type="checkbox"/> Distribution limited to defence departments and defence contractors; further distribution only as approved <input type="checkbox"/> Distribution limited to defence departments and Canadian defence contractors; further distribution only as approved <input type="checkbox"/> Distribution limited to government departments and agencies; further distribution only as approved <input type="checkbox"/> Distribution limited to defence departments; further distribution only as approved <input type="checkbox"/> Other (please specify):			
12. DOCUMENT ANNOUNCEMENT (any limitation to the bibliographic announcement of this document. This will normally correspond to the Document Availability (11). However, where further distribution (beyond the audience specified in 11) is possible, a wider announcement audience may be selected.)			

UNCLASSIFIED

SECURITY CLASSIFICATION OF FORM

13. ABSTRACT (a brief and factual summary of the document. It may also appear elsewhere in the body of the document itself. It is highly desirable that the abstract of classified documents be unclassified. Each paragraph of the abstract shall begin with an indication of the security classification of the information in the paragraph (unless the document itself is unclassified) represented as (S), (C), or (U). It is not necessary to include here abstracts in both official languages unless the text is bilingual).

(U) This technical note presents an improved Kalman filter excisor for dealing with narrowband Gaussian noise. For this type of interference, both envelope and phase vary with time. Since the Kalman filter approach is close to optimum for interferers with constant or very slowly varying envelopes, performance for the narrowband Gaussian noise case will be significantly less than optimum. Ways and means of improving the performance by up to 5 dB are presented. These include the use of an alternate filtering approach to estimate the envelope to counter group delay effects, and phase-smoothing to suppress some of the additional noise caused by temporary loss of lock by the Kalman filter during those instants when the envelope changes sign.

14. KEYWORDS, DESCRIPTORS or IDENTIFIERS (technically meaningful terms or short phrases that characterize a document and could be helpful in cataloguing the document. They should be selected so that no security classification is required. Identifiers, such as equipment model designation, trade name, military project code name, geographic location may also be included. If possible keywords should be selected from a published thesaurus, e.g. Thesaurus of Engineering and Scientific Terms (TEST) and that thesaurus-identified. If it is not possible to select indexing terms which are Unclassified, the classification of each should be indicated as with the title.)

KALMAN FILTER
INTERFERENCE
INTERFERENCE SUPPRESSION
EXCISION
SPREAD SPECTRUM

UNCLASSIFIED

SECURITY CLASSIFICATION OF FORM